*Radio Science*, Volume 31, Number 6, Pages 1733–1742, November–December 1996

# Scattering and absorption of *E*- and *H*-polarized plane waves by a circularly curved resistive strip

A. I. Nosich
Institute of Radiophysics and Electronics, Ukrainian Academy of Sciences, Kharkiv

Y. Okuno and T. Shiraishi
Department of Electrical Engineering and Computer Science, Kumamoto University, Kumamoto, Japan

**Abstract.** An analytical-numerical method of analysis is presented for two-dimensional wave diffraction by an open circular resistive strip. The method is based on the dual series equations regularization approach and results in algorithms with accuracy limited only by a computer's digital precision. Scattering and absorption cross sections are computed as functions of frequency for lossless and lossy strips.

## 1. Introduction

The scattering of waves from zero-thickness, perfectly conducting strips and surfaces has been a traditional topic in diffraction theory. However, an imperfect structure such as a resistive or conductive strip is obviously of greater practical interest. Following *Senior* [1978] and *Senior and Volakis* [1987], a combination of resistive and conductive sheets can be used for simulating magnetodielectric layers and impedance surfaces. Due to a known duality, an electrically resistive (conductive) strip is similar to magnetically conductive (resistive) one. Hence it is sufficient to analyze the scattering of electrically ($E$) and magnetically ($H$) polarized waves by an electrically resistive strip. Although flat resistive strips have been studied in a number of papers, the curved ones seem so far to have avoided any numerical analysis. An analytical high-frequency study, however, was reported by *Büyükaksoy and Uzğoren* [1988].

The scattering geometry is shown in Figure 1. A circularly curved strip $M$ of radius $a$, angular width $2\theta_{ap}$, and aspect angle $\phi_0$ is exposed to an excitation by a plane $E$- or $H$-polarized wave propagating along the $x$ axis. The resistivity is assumed to be $R_s = Z_0 R$, where $Z_0$ is the free space impedance. Following *Senior* [1979] and *Bouchitté and Petit* [1989], we can imply that for a realistic metallic surfaces, $R = (h\sigma)^{-1}$, where $\sigma$ is the conductivity and $h$ is the thickness of an actual strip, which is simulated by a zero-thickness one. Also, for a thin sheet of dielectric, $R = i/[kh(\varepsilon - 1)]$, and a lossless scatterer is realized if we set $\mathrm{Re}\, R = 0$.



Paper number 96RS02183.
0048-6604/96/96RS-02183$11.00

Canonical scattering geometry like this has been studied previously by many authors assuming a perfect electric conductor (PEC). A commonly accepted way to obtain a numerical solution to such a problem was initiated by *Zakharov and Pimenov* [1979] and also by *Beren* [1983] who treated the electric field integral equation (EFIE) (or the magnetic field integral equation) by the method of moments (MOM). Later, *Mautz and Harrington* [1988, 1989] developed a modified MOM procedure that remained stable in case of a narrow slot, to study the resonances. *Goggans and Shumpert* [1991] and also *Sadigh and Arvas* [1993] extended this approach to solve the problem of dielectric-filled two-dimensional (2-D) cavities of more arbitrary shape. A close relative to the MOM called a modified point-matching method was used by *Hosono* [1991] to study the transient response of a slitted PEC cylinder.

Another numerical approach involves greater analytical work but offers certain advantages. *Sologub et al.* [1967] were the first to reduce the scattering by an open circular cylinder with $N$ periodic longitudinal slots to a set of dual series equations, where they made use of the so-called Riemann-Hilbert problem (RHP) solution to obtain a regularized matrix equation. This article and a following paper by *Koshparenok et al.* [1971] started the series of Soviet papers on slitted circular PEC cylinders analyzed by the method-of-regularization (MOR). *Nosich* [1978], *Johnson and Ziolkowski* [1984], and *Ziolkowski and Grant* [1987] used this approach later to analyze numerically the far-field characteristics and surface

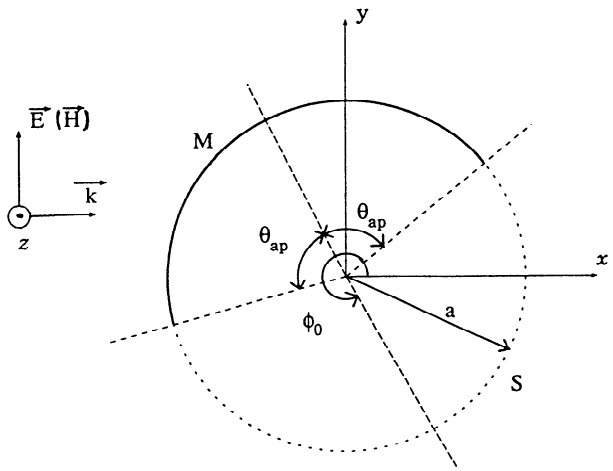


**Figure 1.** Scattering geometry of a circularly curved strip.

current distribution for the slitted circular cylinder. A partial list of relevant Soviet papers was given by *Nosich* [1993] together with some extentions of the method. Radar cross section (RCS) analysis of lossy-material-lined and coated slitted PEC cavities was presented by *Çolak et al.* [1993, 1995].

Here a note should be made on the relation between the MOM and MOR solutions. Generally, MOR is considered to be more accurate but complicated and restricted to circular geometries while MOM as simpler and more universal. The bridge between the two approaches has been established in an important paper by *Gestrina* [1969], who obtained the same matrix equation as that of MOR without solving the RHP, but only through careful use of certain properties of singular integral equations. The key is to split the kernel of EFIE by extracting the logarithmic part of the Green's function and to use the set of orthogonal eigenfunctions of this partial kernel as the basis and testing functions in a Galerkin-like procedure. Taking account of this, MOR can be understood as a sophisticated version of MOM, due to the judicious choice of expansion functions.

In contrast to MOM, MOR is free from any problems of relative convergence, stability, or accuracy failure in the vicinity of resonance [see *Hower et al.*, 1993]. It works equally well for an arbitrary strip (or slot) width and orientation and for the surface current, near-field and far-field calculations. The general relations as energy conservation and reciprocity are satisfied in term-by-term manner; the errors in such relations are at the level of digital precision. The applicable range of frequency is sufficiently wide and is limited only by the memory available on a computer. Moreover, the memory size requirement is not severe: because the MOR results in a matrix equation of the Fredholm second kind, it can be solved by a conjugate-gradient method instead by matrix inversion.

The aim of this paper is to present an efficient MOR solution to resistive strip scattering. Mathematically, the problem of excitation by a known $E$- or $H$-polarized field (time dependence $e^{-iwt}$ is assumed) can be formulated as follows. Define the $z$ component of the total electric or magnetic field as

$$U = U^{in} + U^{sc} \tag{1}$$

assuming that the $U^{in}$ is the field in the absence of the strip. Then the scattered field function must solve the 2-D Helmholtz equation

$$(\nabla^2 + k^2)U^{sc}(\mathbf{r}) = 0, \tag{2}$$

where $\mathbf{r} \in R^2/M$, $k = w/c$, $\operatorname{Im} k = 0$, with a set of boundary, edge, and radiation condition:

$$\left(\frac{\partial}{\partial r} \pm i\alpha\right)U = 0, \qquad \mathbf{r} \in M_{\pm}, \tag{3}$$

$$\int_B (k^2|U^{sc}|^2 + |\nabla U^{sc}|^2)\, dr < \infty, \qquad \forall B \subset R^2, \tag{4}$$

$$U^{sc}(\mathbf{r}) \sim \Phi^{sc}(\phi)(2/i\pi kr)^{1/2}e^{ikr}, \qquad r \to \infty, \tag{5}$$

where $\alpha = k/R$ in the $E$ polarization and $\alpha = kR$ in the $H$ polarization; and $M_{\pm}$ denote the outer and the inner surface of the strip, respectively. To simulate an electrically resistive strip, we need to add the condition of tangential $E$ field continuity across the strip, i.e.,

$$[E]_{-}^{+} = 0 \tag{6}$$

or

$$[\partial H/\partial r]_{-}^{+} = 0, \tag{7}$$

depending on the polarization.

We shall obtain regularized matrix equations for $E$ polarized (section 2) and for $H$-polarized (section 3) scattering. In proceeding with analysis, an important step is to reduce the original problem, equations (1)–(7), to the dual series equations. Partial inversion of the equations may be done based on the inverse Fourier transformation in the $E$-polarized case. In the

$H$-polarized case, however, we need a RHP-like treatment that is similar to one employed in the solution of scattering by a PEC strip. Verification of the algorithm is presented. Sample numerical results are given for lossless and lossy circular strips. The results which include total, backscattering, and absorption cross sections.

## 2. E Wave Scattering and Absorption

The general scheme of treatment follows one given by *Senior* [1978]. We start by seeking the scattered field as a single-layer potential with unknown density function $X(\mathbf{r}')$

$$E^{sc}(\mathbf{r}) = \int_M X(\mathbf{r}')G_0(\mathbf{r}, \mathbf{r}')\, d\mathbf{r}', \tag{8}$$

where $\mathbf{r}'$ is a point on $M$ and the kernel function of such a representation is the 2-D Green's function, i.e.,

$$G_0(\mathbf{r}, \mathbf{r}') = \frac{i}{4} H_0^{(1)}(k|\mathbf{r} - \mathbf{r}'|). \tag{9}$$

Thus the original problem is reduced to the search for the surface current density function $X(\mathbf{r}')$. By using the boundary condition (3) and the jump condition (6), we obtain an EFIE as

$$X(\mathbf{r}) + 2i\alpha \int_M X(\mathbf{r}')G_0(\mathbf{r}, \mathbf{r}')\, d\mathbf{r}' = -2i\alpha E^{in}(\mathbf{r}), \qquad \mathbf{r} \in M. \tag{10}$$

Note that because the kernel in (10) has a logarithmic singularity, this integral equation is of the Fredholm second kind provided that $R \neq 0$. Hence it can be solved by a direct MOM-like algorithm. One frequently met problem in MOM-based solutions is the failure in the case of a narrow slot (or strip). To overcome this difficulty, we treat the scatterer as a complete circle, and redefining the function $X(\phi')$ to be zero off the actual strip, we extend the integration in (10) from $M$ to an entire circle ($r = a$, $0 \leq \phi \leq 2\pi$).

By expanding the current density and the kernel function in terms of angular exponents, we arrive at the representations

$$X(\mathbf{r}') \equiv X(\phi') = \frac{2}{i\pi a} \sum_{n=-\infty}^{\infty} x_n e^{in\phi'} \tag{11}$$

$$E^{sc}(\mathbf{r}) = \sum_{n=-\infty}^{\infty} x_n e^{in\phi} \begin{cases} J_n(ka)H_n^{(1)}(kr), & r > a \\ J_n(kr)H_n^{(1)}(ka), & r > a \end{cases}. \tag{12}$$

After expanding similarly the incident field and calculating the integral in (10), we obtain the following dual series equations:

$$\sum_{n=-\infty}^{\infty} x_n \left( \frac{-1}{\pi a \alpha} + J_n H_n \right) e^{in\phi} = -\sum_{n=-\infty}^{\infty} i^n J_n e^{in\phi}, \qquad |\phi - \phi_0| < \theta_{ap} \tag{13}$$

$$\sum_{n=-\infty}^{\infty} x_n e^{in\phi} = 0, \qquad \theta_{ap} < |\phi - \phi_0| \leq \pi \tag{14}$$

where the argument of cylindrical functions $J_n$ and $H_n \equiv H_n^{(1)}$ is $ka$. Note that the appearance of (14) is the price of simplifying the shape of the scatterer. The expected gain is that the solution is equally efficient for any value of $\theta_{ap}$ and $\phi_0$. In addition, the condition of limited stored energy in any finite domain (4), if applied to a circle $r \leq a$ for example, yields a requirement that

$$\sum_{n=-\infty}^{\infty} |x_n|^2 (|n| + 1)^{-1} < \infty. \tag{15}$$

Due to the large-$n$ behavior $J_n H_n \sim O(|n|^{-1})$, the dual series equations, (13) and (14), can be subjected to the partial Fourier-inversion procedure. This results in a matrix equation of the Fredholm second kind:

$$(I - A^E)\tilde{X} = B^E, \tag{16}$$

where

$$I_{mn} = \delta_{mn}, \tag{17}$$

$$A_{mn}^E = (ka/R)[(|n| + 1)/(|m| + 1)]^{1/2} J_n H_n S_{mn}(\theta_{ap}, \phi_0)$$

$$\tilde{x}_n = x_n (|n| + 1)^{-1/2}, \tag{18}$$

$$B_m^E = (ka/R)(|m| + 1)^{-1/2} \sum_{n=-\infty}^{\infty} i^n J_n S_{mn}(\theta_{ap}, \phi_0).$$

The angular coefficients are given by

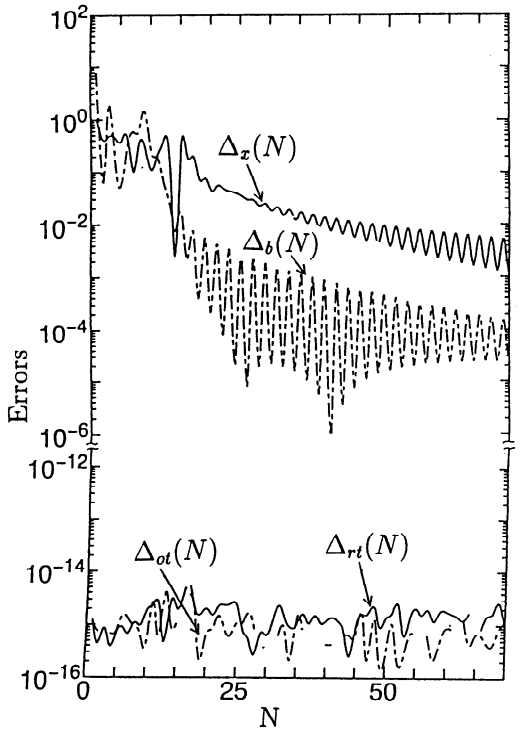


**Figure 2.** Computational errors as functions of the matrix truncation number for $E$ polarization, $ka = 10$, $R = -i0.1$, $\theta_{ap} = 90°$, and $\phi_0 = 170°$.

$$S_{mn} = e^{i(n-m)\phi_0} \begin{cases} \dfrac{\sin[(n-m)(\theta_{ap}-\pi)]}{n-m}, & m \neq n \\ \theta_{ap} - \pi, & m = n \end{cases} \tag{19}$$

Investigation of the large-index behavior of the elements $A^E_{mn}$ reveals that

$$A^E_{mn} = O[(|m-n|+1)^{-1}|mn|^{-1/2}]. \tag{20}$$

Hence independently of the angular parameters $\theta_{ap}$ and $\phi_0$, the electrical radius $ka$, or of the resistivity $R$, we have $\Sigma_{m,n=-\infty}^{\infty}|A^E_{mn}|^2 < \infty$. This guarantees that the needed solution exists, is unique, and can be approximated by solving a truncated matrix equation. The estimation (20) guarantees also convergence of the series (15), and hence the condition (4) is satisfied.

The quantities of practical interest are the far-field scattering pattern $\Phi^{sc}(\phi)$, the total scattering cross section $\sigma_{sc}$, the backscattering RCS $\sigma_b$, and the absorption cross section $\sigma_{ab}$ (provided that Re $R >$ 0). We find that the first three are given, respectively, by the following series expressions:

$$\Phi^{sc} = \sum_{n=-\infty}^{\infty} x_n(-i)^n J_n e^{in\phi}, \tag{21}$$

$$\sigma_{sc} \equiv \frac{2}{\pi k}\int_0^{2\pi} |\Phi^{sc}(\phi)|^2\, d\phi = \frac{4}{k}\sum_{n=-\infty}^{\infty} |x_n|^2 J_n^2, \tag{22}$$

$$\sigma_b \equiv \frac{4}{k}|\phi^{sc}(\pi)|^2 = \frac{4}{k}\left|\sum_{n=-\infty}^{\infty} x_n i^n J_n\right|^2. \tag{23}$$

Under a plane wave incidence, the total scattering cross section of a localized scatterer has to satisfy the optical theorem (power conservation law):

$$\sigma_{ext} \equiv \sigma_{sc} + \sigma_{ab} = -\frac{4}{k}\,\mathrm{Re}\,\Phi^{sc}(0). \tag{24}$$

The scattering pattern, in addition, should meet the reciprocity theorem, which in our case may be written as

$$\Phi^{sc}(0, \phi_0) = \Phi^{sc}(0, \pi - \phi_0). \tag{25}$$

These relations can be used for checking the numerical algorithm in order to avoid rough mistakes. Besides, (24) may be used for calculating the absorption provided that $\sigma_{sc}$ and $\Phi^{sc}(0)$ have been computed.

Figure 2 gives the understanding of the main features of the numerical algorithm based on the equations presented above. The truncation errors for the surface current and the RCS of a lossless strip are defined, respectively, as functions of a given truncation order $N$ by

$$\Delta_x(N) = \frac{\max|x_n^N - x_n^{N+1}|}{\max|x_n^N|}, \qquad \Delta_b(N) = \frac{|\sigma_b^N - \sigma_b^{N+1}|}{\sigma_b^N}. \tag{26}$$

The accuracy in satisfying the general relations (24) and (25) is estimated by

$$\Delta_{ot}(N) = 2\frac{|k\sigma_{ext}^N + 4\,\mathrm{Re}\,\Phi^{sc,N}(0)|}{|k\sigma_{ext}^N - 4\,\mathrm{Re}\,\Phi^{sc,N}(0)|},$$
$$\Delta_{rt}(N) = 2\frac{|\Phi^{sc,N}(0, \phi_0) - \Phi^{sc,N}(0, \pi - \phi_0)|}{|\Phi^{sc,N}(0, \phi_0) + \Phi^{sc,N}(0, \pi - \phi_0)|}. \tag{27}$$

One can see that by taking the truncation number as $N \geq (1 + |R|^{-1/2})ka + 10$, the relative accuracy of the surface current computation is guaranteed to 0.01, while that of the RCS is 0.001. This rule is applied when computing the scattering characteristics

as functions of frequency (see Figures 3 and 4). At the same time, the power conservation and the reciprocity are satisfied in a numerically exact manner: the errors are determined only by the digital precision of the computer. Moreover, both seem to be satisfied in a term-by-term manner; however, this is difficult to prove analytically.

In Figures 3 and 4 the scattering and absorption cross sections as functions of the normalized frequency $ka$ are presented for a semicircular strip/shell. All the plots are normalized by the corresponding high-frequency limit value for a closed PEC cylinder,

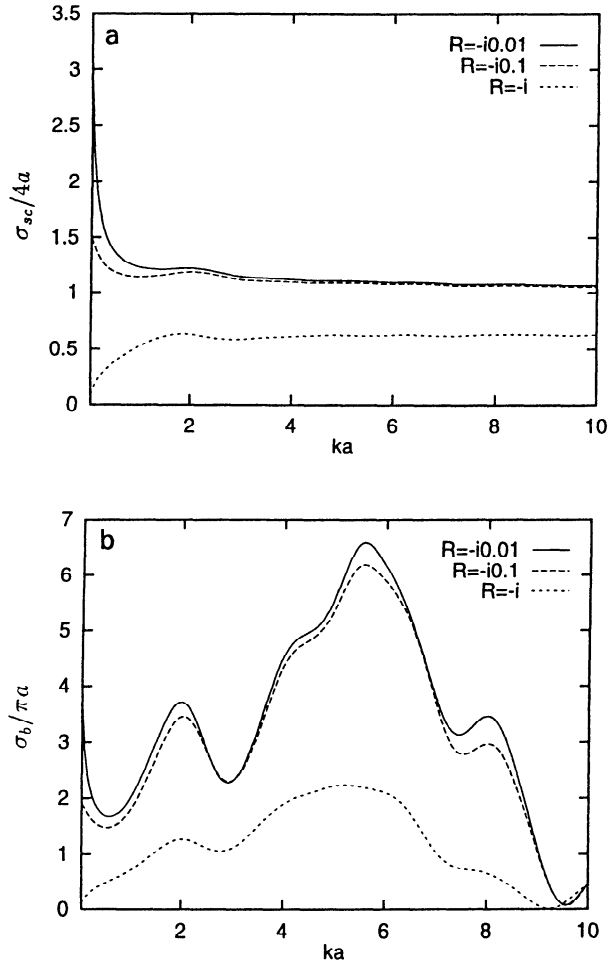


**Figure 3.** Lossless resistive strip scattering characteristics in $E$ polarization: (a) total scattering cross section $\sigma_{sc}/4a$, and (b) backward radar scattering cross section $\sigma_b/\pi a$, as functions of normalized frequency $ka$. Solid curves correspond to a resistivity $R = -i0.01$, dashed curves correspond to $R = -i0.1$, and dotted curves correspond to $R = -i$. Strip geometry is $\theta_{ap} = 90°$ and $\phi_0 = 170°$.

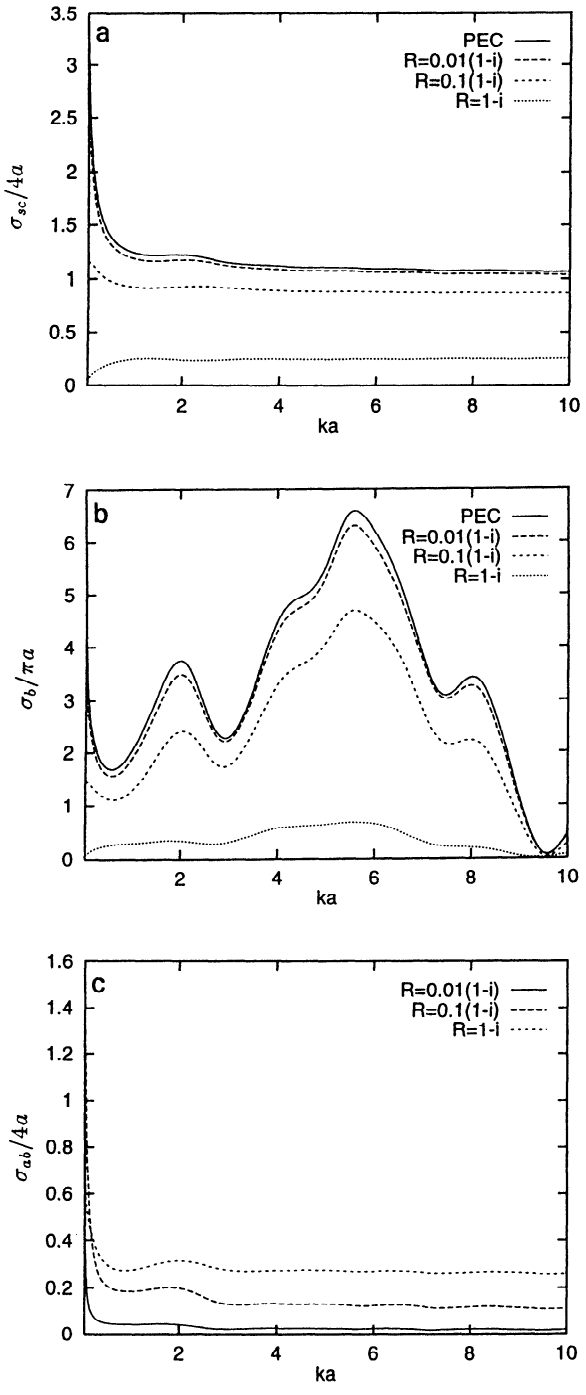


**Figure 4.** Lossy resistive strip characteristics in $E$ polarization: (a) total scattering cross section $\sigma_{sc}/4a$, (b) backward radar scattering cross section $\sigma_b/\pi a$, and (c) absorption cross section $\sigma_{ab}/4a$ as functions of normalized frequency $ka$. Solid curves are for a PEC strip $R = 0$, long-dashed curves are for $R = 0.01(1 - i)$, short-dashed curves are for $R = 0.1(1 - i)$, and dotted curves are for $R = 1 - i$. Strip geometry is $\theta_{ap} = 90°$ and $\phi_0 = 170°$.

which is $4a$ for the total scattering and the absorption cross section, and $\pi a$ for the RCS. The values of the resistivity were taken to be of the order of 0.01, 0.1, and 1 in order to cover the range of practical interest, and a comparison with the PEC case was made (see Figures 4a and 4b) based on a separate treatment. Generally, no resonances are seen in the total cross section, but the RCS and the absorption cross section (to a lesser extent) do show the resonances, which are suppressed if the loss (Re $R$) becomes greater.

## 3. H Wave Scattering and Absorption

The treatment is similar, in part, to the previous case. We seek the scattered field as a double-layer potential [*Senior*, 1978], with an unknown density function $Y(\mathbf{r}')$:

$$H^{sc}(\mathbf{r}) = \int_M Y(\mathbf{r}') \frac{\partial}{\partial r'} G_0(\mathbf{r}, \mathbf{r}')\, d\mathbf{r}'. \tag{28}$$

The kernel function here is the outer normal derivative of the 2-D Green's function $G_0$. Thus the original problem is reduced to the search for the surface current density function $Y(\mathbf{r}')$. By using the boundary condition (3) and the jump relation (7), we obtain an EFIE as

$$i\alpha Y(\mathbf{r}) + 2\frac{\partial}{\partial r} \int_M Y(\mathbf{r}') \frac{\partial}{\partial r'} G_0(\mathbf{r}, \mathbf{r}')\, d\mathbf{r}', \tag{29}$$

$$\mathbf{r} \in M.$$

Note that (29) is a hypersingular equation and hence any direct MOM-like algorithm will have at best a questionable convergence and stability. Similarly to the $E$-polarized case, we treat the scatterer as the circular one assuming the function $Y(\phi')$ to vanish off the actual strip.

Expanding the current density, the kernel function, and the incident field in terms of angular exponents, we have expressions like

$$Y(\mathbf{r}') \equiv Y(\phi') = \frac{2}{i\pi ka} \sum_{n=-\infty}^{\infty} y_n e^{in\phi'}, \tag{30}$$

$$H^{sc}(\mathbf{r}) = \sum_{n=-\infty}^{\infty} y_n e^{in\phi} \begin{cases} J_n'(ka) H_n^{(1)}(kr), & r > a \\ J_n(kr) H_n^{(1)'}(ka), & r < a \end{cases}. \tag{31}$$

Equation (29) is thus modified to the dual series equations

$$\sum_{n=-\infty}^{\infty} y_n \left( \frac{\alpha}{\pi k^2 a} + J_n' H_n' \right) e^{in\phi} = -\sum_{n=-\infty}^{\infty} i^n J_n' e^{in\phi}, \tag{32}$$

$$|\phi - \phi_0| < \theta_{ap}$$

$$\sum_{n=-\infty}^{\infty} y_n e^{in\phi} = 0, \qquad \theta_{ap} < |\phi - \phi_0| \le \pi \tag{33}$$

Here the prime denotes differentiation with respect to the argument, which is $ka$ and is omitted. The condition of limited stored energy (4) yields a requirement that

$$\sum_{n=-\infty}^{\infty} |y_n|^2 (|n| + 1) < \infty. \tag{34}$$

Unlike the $E$-polarized case, the dual series equations, (32) and (33) cannot be inverted partially by the inverse Fourier transformation because of the large-$n$ behavior $J_n' H_n' \sim O(|n|)$. Instead, they can be handled by an RHP-like procedure, which is similar to one employed in the PEC case. The result is a matrix equation of the Fredholm second kind:

$$(I - A^H) = B^H, \tag{35}$$

where

$$I_{mn} = \delta_{mn}, \qquad A_{mn}^H = K_n(ka, R) T_{mn}(\theta_{ap}, \phi_0), \tag{36}$$

$$K_n(ka, R) = ikaR + |n| + i\pi(ka)^2 J_n' H_n', \tag{37}$$

$$B_m^H = i\pi(ka)^2 \sum_{n=-\infty}^{\infty} i^n J_n' T_{mn}(\theta_{ap}, \phi_0). \tag{38}$$

The angular coefficients are the same as that for the $H$ wave scattering from a perfectly conducting open circular strip [*Nosich*, 1993], i.e.,

$$T_{mn} = (-1)^{n-m} \exp[i(n-m)\phi_0] \cdot \frac{P_{m-1}(u) P_n(u) - P_{n-1}(u) P_m(u)}{2(m-n)}, \tag{39a}$$

$$m \neq n$$

$$T_{mn} = (-1)^{n-m} e^{i(n-m)\phi_0} \frac{1}{2|n|} \sum_{s=0}^{|n|} q_{|n|-s}(u) P_{|n|-s-1}(u), \tag{39b}$$

$$m = n \neq 0$$

$$T_{mn} = (-1)^{n-m} \exp[i(n-m)\phi_0] - \ln \tfrac{1}{2}(1 + \cos\theta_{ap}), \tag{39c}$$

$$m = n = 0$$

where $q_0 = 1$, $q_1 = -u_1, \cdots, q_s = P_s - 2uP_{s-1}(u) + P_{s-2}(u)$, and $P_s(u)$ are the Legendre polynomials of the argument $u = \cos\theta_{ap}$.

Note that the leading contribution to the $K_n$ coefficient in (37) comes from the term $ikaR$, which remains constant as $|n| \to \infty$, while the last two terms together decay as $O(k^2a^2/|n|)$. Hence it is the large-index behavior of the $T_{mn}$ coefficient,

$$T_{mn} = O[(|m-n|+1)^{-1}|mn|^{-1/2}], \tag{40}$$

that ensures the Fredholm nature of (35) and also the needed edge behavior.

Far-field scattering pattern, scattering cross-sections, and general field relations are given by the expressions similar to (21)–(25), where $x_n$ and $J_n$ should be replaced by $y_n$ and $J'_n$.

To illustrate the main features of the $H$-polarized case algorithm, relative errors in computing the current and the RCS and those of power conservation and reciprocity for a lossless strip are shown in Figure 5 as functions of the number of matrix truncation. One can see that by setting the number as $N \geq (1 + |R|^{1/2})ka + 10$, the relative errors in the surface current and the RCS, respectively, are less than 0.01 and 0.001.

This rule is applied in computation of frequency characteristics of a semicircular strip/shell (see Figures 6 and 7). Note that the power conservation and the reciprocity are satisfied again in a numerically exact manner. A resistive curved strip, in general, shows stronger resonances when illuminated by an $H$-polarized plane wave than when illuminated by an $E$-polarized wave. This is similar to the PEC case and is explained by the circumferential flow of the surface current. In these figures, plots for a corresponding PEC obstacle are not shown just because they coincide with the plots for the $|R| = 0.01$ case. The resonances are well observable in the total, backscattering, and absorption cross section.

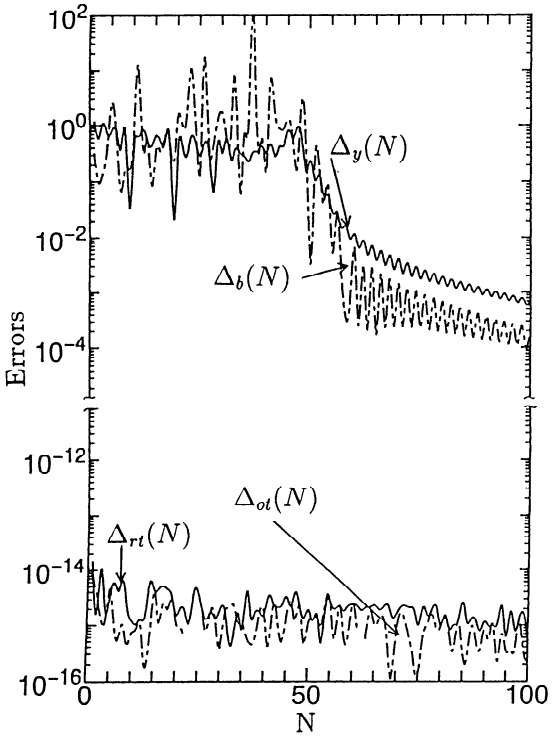


**Figure 5.** Computational errors as functions of the matrix truncation number, for $H$ polarization, $ka = 50$, $R = -i0.1$, $\theta_{ap} = 90°$, and $\phi_0 = 170°$.

Due to the resonance, the overall absorption can be enhanced in spite of a relatively small surface loss. The lowest frequency resonance is known as the Helmholtz resonance [see *Nosich*, 1978; *Ziolkowski and Grant*, 1987; *Çolak et al.*, 1995]. The regularized character of (35) offers a way of finding an approximate analytical solution provided that the norm of the $A^H$ operator is small. This is the case if the electrical dimension of the strip tends to zero. Hence an asymptotic eigenvalue analysis of (35), assuming $ka \to 0$, results in the following complex resonant frequency

$$k_H a = k_0 a \left\{ 1 + \frac{i}{4}(k_0 a)^2 \cdot \left[ 1 - \frac{iR/2}{(-2^{-1}\ln^{-1}\sin(\pi - \theta_{ap})/2 - R^2/4)^{1/2}} \right] \right\}, \tag{41}$$

where

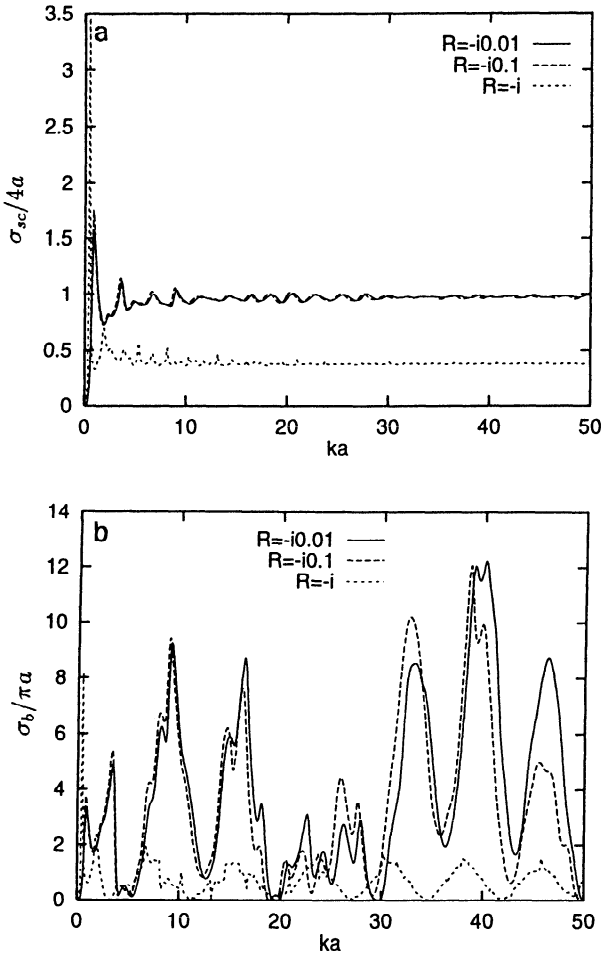


**Figure 6.** Lossless resistive strip scattering characteristics in $H$ polarization: (a) total scattering cross section $\sigma_{sc}/4a$, and (b) backward radar scattering cross section $\sigma_b/\pi a$, as functions of normalized frequency $ka$. Solid curves correspond to a resistivity $R = -i0.01$, dashed curves correspond to $R = -i0.1$, and dotted curves correspond to $R = -i$. Strip geometry is $\theta_{ap} = 90°$ and $\phi_0 = 170°$.

$$k_0 a = \left( -\tfrac{1}{2} \ln^{-1} \sin \frac{\pi - \theta_{ap}}{2} - \tfrac{1}{4} R^2 \right)^{1/2} - \frac{i}{2} R. \qquad (42)$$

One may see that the frequency given by (42) is shifted toward a lower frequency range than in the PEC case. Its $Q$ factor is now governed together by the radiation loss via the $\theta_{ap}$-dependent terms and the ohmic loss via the real part of the resistivity $R$.

## 4. Conclusions

Method of regularization (MOR) numerical solutions have been presented for the $E$- and the $H$-

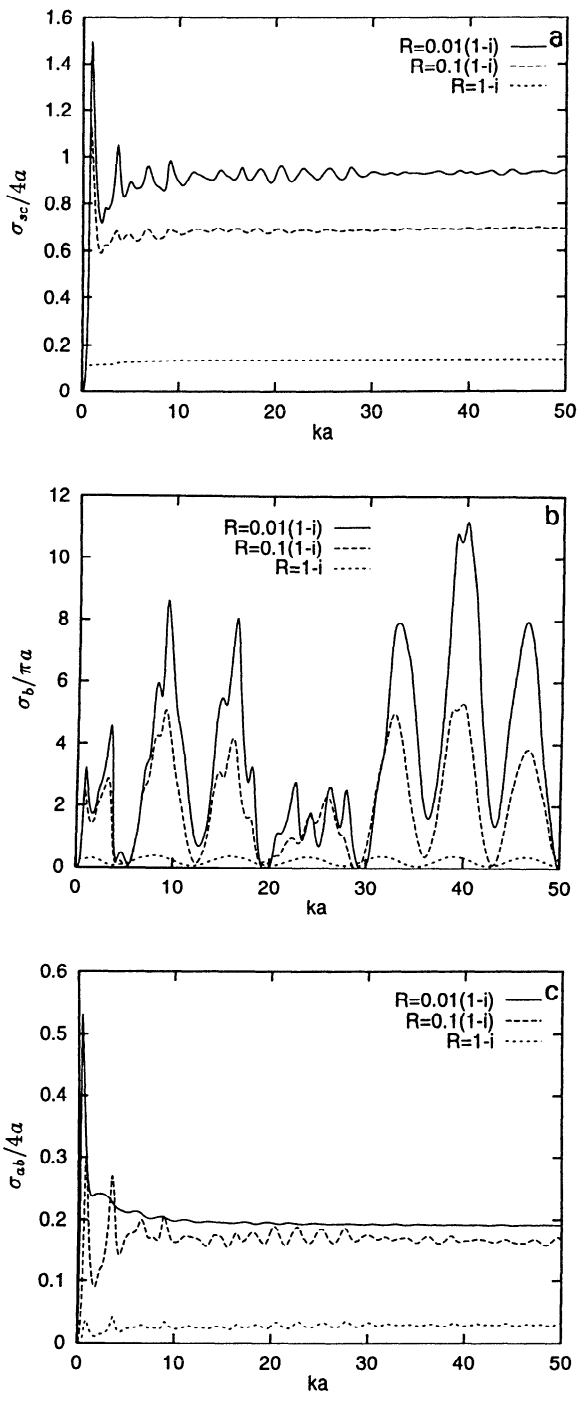


**Figure 7.** Lossy resistive strip characteristics in $H$ polarization: (a) total scattering cross section $\sigma_{sc}/4a$, (b) backward radar scattering cross section $\sigma_b/\pi a$, and (c) absorption cross section $\sigma_{ab}/4a$ as functions of normalized frequency $ka$. Solid curves are for $R = 0.01(1 - i)$, long-dashed curves are for $R = 0.1(1 - i)$, and short-dashed curves for $R = 1 - i$. Strip geometry is $\theta_{ap} = 90°$ and $\phi_0 = 170°$.

polarized wave scattering from an open circularly curved resistive strip. The solutions are equally efficient for an arbitrary angular width and orientation of the strip. The range of the computable electrical size $ka$ and the resistivity $|R|$ is decided only by the computer used: a typical matrix size $N = ka(1 + |R|^{\pm 1/2}) + 10$ is needed for 3-digit accuracy for the RCS prediction in the $H/E$ polarization.

It may be interesting to compare the results with that in the PEC case. In the $H$ polarization, this is done by setting $R = 0$. In the $E$ polarization, however, this limit is not directly accessible because the matrix equation loses the regularized character there. Nevertheless, a numerical solution shows that if the normalized resistivity is sufficiently small, say, $|R| < 10^{-3}$, a perfect agreement with the PEC case is seen except for a narrow quasi-static range. The root of the difference between the $E$- and $H$-polarized case may be considered as follows: In the $H$-polarized problem, it is the term $\alpha = kR$ that perturbes the PEC (Neumann) boundary condition; while in the $E$-polarized problem, it is the ratio $1/\alpha = R/k$ that is perturbing the PEC (Dirichlet) condition. Hence the latter perturbation is singular: at the static limit $k \to 0$ it turns the $E$-polarized boundary condition into the Neumann condition.

The numerical results presented show that a lossless resistive shell causes a series of scattering resonances, stronger in the $H$-polarized case, but not so sharp as in the PEC case because of the partial transparency. A lossy resistive shell behaves like a resonant absorber. In terms of the absorption cross-section, a tenfold reduction in the surface loss can be more than compensated by tuning the geometry to a resonance. The RCS resonances, which are well observed in a PEC cavity-backed aperture frequency scans, can efficiently be suppressed by introducing a resistive loss. In the $H$ polarization case, the Helmholtz resonance occurs at a lower frequency than in the PEC case. Due to the regularized character of the matrix equation, an explicit expression for the shifted complex resonance frequency has been obtained.

## References


Beren, J. A., Diffraction of an H-polarized electromagnetic wave by a circular cylinder with an infinite axial slot, *IEEE Trans. Antennas Propag., AP-31*(3), 419–425, 1983.

Bouchitté, G., and R. Petit, On the concepts of a perfectly conducting material and of a perfectly conducting and infinitely thin screen, *Radio Sci., 24*(1), 13–26, 1989.

Büyükaksoy, A., and G. Uzğoren. Diffraction of high-frequency waves by cylindrically curved surface with different face impedances, *IEEE Trans. Antennas Propag., AP-36*(4), 690–695, 1988.

Çolak, D., A. I. Nosich, and A. Altintaş, RCS study of cavity-backed apertures with inner and outer material loading: The case of $E$-polarization, *IEEE Trans. Antennas Propag., 41*(11), 1551–1559, 1993.

Çolak, D., A. I. Nosich, and A. Altintaş, RCS study of cavity-backed apertures with inner and outer material loading: The case of $H$-polarization, *IEEE Trans. Antennas Propag., 43*(5), 440–447, 1995.

Gestrina, G. N., Diffraction of a plane electromagnetic wave from metallic grating (in Russian), *Radiotekhnika Kharkov, 10*, 3–14, 1969.

Goggans, P. M., and T. H. Shumpert, Backscatter RCS for TE and TM excitation of dielectric-filled cavity-backed apertures in 2-D bodies, *IEEE Trans. Antennas Propag., 39*(8), 1224–1227, 1991.

Hosono, H., Transient responses of electromagnetic waves scattered by a circular cylinder with longitudinal slots, *Trans. Inst. Electron. Inf. Commun. Eng. E, 74*(9), 2864–2869, 1991.

Hower, G. L., R. G. Olsen, J. D. Earls, and J. B. Schneider, Inaccuracies in numerical calculation of scattering near natural frequencies of penetrable objects, *IEEE Trans. Antennas Propag., 41*(7), 982–986, 1993.

Johnson, W. A., and R. W. Ziolkowski, The scattering of H-polarized plane wave from an axially slotted infinite cylinder: a dual series approach, *Radio Sci., 19*(1), 275–291, 1984.

Koshparenok, V. N., and V. P. Shestopalov, Diffraction of a plane electromagnetic wave by a circular cylinder with a longitudinal slot, *USSR Comput. Math. Math. Phys.*, Engl. Transl., *11*(3), 222–243, 1971.

Mautz, J. R., and R. F. Harrington, Electromagnetic penetration into a conducting circular cylinder through a narrow slot, TM case, *J. Electromagn. Waves Appl., 2*(3/4), 269–293, 1988.

Mautz, J. R., and R. F. Harrington, Electromagnetic penetration into a conducting circular cylinder through a narrow slot, TE case, *J. Electromagn. Waves Appl., 3*(4), 307–336, 1989.

Nosich, A. I., About the effect of resonances on the scattering characteristics of non-closed cylinder (in Russian), *Radiotekh. Elektron. Moscow, 23*(8), 1733–1737, 1978.

Nosich, A. I., Green's function—Dual series approach in wave scattering from combined resonant scatterers, in *Analytical and Numerical Methods in Electromagnetic Wave Theory*, edited by M. Hashimoto, M. Idemen, and O. A. Tretyakov, pp. 419–469, Sci. House, Tokyo, 1993.

Sadigh, E., and E. Arvas, Electromagnetic penetration into a dielectric-filled conducting shell of arbitrary cross-

section through an infinite slot: TE case, *Arch. Elektrotech. Uebertrat.*, *47*(3), 166–169, 1993.

Senior, T. B. A., Some problems involving imperfect half planes, in *Electromagnetic Scattering*, edited by P. L. E. Uslenghi, pp. 185–219, Academic, San Diego, Calif., 1978.

Senior, T. B. A., Backscattering from resistive strips, *IEEE Trans. Antennas Propag.*, *AP-27*(6), 808–813, 1979.

Senior, T. B. A., and J. L. Volakis, Sheet simulation of a thin dielectric layer, *Radio Sci.*, *22*(7), 1261–1272, 1987.

Sologub, V. G., O. A. Tretyakov, S. S. Tretyakova, and V. P. Shestopalov, Excitation of an open structure of the "squirrel cage" type by a circularly moving charge (in Russian), *Zh. Tech. Fiz.*, *12*(10), 1923–1931, 1967.

Zakharov, E. V., and Y. V. Pimenov, Numerical analysis of diffraction of electromagnetic waves by an open circular-cylindrical surface, *Radiophys. Quantum Electron.*, Engl. Transl., *22*, 426–431, 1979.

Ziolkowski, R. W., and J. B. Grant, Scattering from cavity-backed apertures: The generalized dual series solution of the concentrically loaded *E*-pol slit cylinder problem, *IEEE Trans. Antennas Propag.*, *AP-35*(5), 504–528, 1987.

A. I. Nosich, Institute of Radiophysics and Electronics, Ukrainian Academy of Sciences, Kharkiv 310085, Ukraine. (e-mail: alex@emt.kharkov.ua).

Y. Okuno and T. Shiraishi, Department of Electrical and Computer Engineering, Kumamoto University, Kurokami 2-39-1, Kumamoto 860, Japan. (e-mail: okuno@gpo.kumamoto-u.ac.jp)

(Received September 15, 1995; revised June 11, 1996; accepted June 24, 1996.)